AIAA JOURNAL
Vol. 31, No. 3, March 1993

Laser Selection Criteria for OH Fluorescence Measurements in Supersonic Combustion Test Facilities

T. M. Quagliaroli,* G. Laufer,† R. H. Krauss,‡ and J. C. McDaniel Jr.†
University of Virginia, Charlottesville, Virginia 22903

The limitations of the application of dye laser and narrow-band tunable KrF excimer laser systems to OH planar laser-induced fluorescence measurements in supersonic combustion test facilities are examined. Included in the analysis are effects of signal strength, collisional quenching, beam absorption, and fluorescence trapping on achievable measurement accuracy using several excitation and detection options for either of the two laser systems. Dye based laser systems are found to be the method of choice for planar imaging when the line integral of OH concentration along the incidence or detection paths is less than 10^{16} cm/cm^3, whereas the KrF based systems provide significant reduction in measurement ambiguity when either concentration line integral is in excess of 10^{16} cm/cm^3.

Introduction

THE development of a supersonic combustion ramjet (scramjet) engine will depend heavily on computational codes.[1] Validation of these codes requires spatially resolved and accurate experimental data on the mixing and combustion of hydrogen in high stagnation temperature supersonic flow facilities. Planar laser-induced fluorescence (PLIF) techniques are nonintrusive and usually provide the level of signal necessary for high signal-to-noise ratio imaging in the mixing and reacting regions as well as high sensitivity to density and temperature of the probed molecules.[2] Furthermore, single shot temperature and density measurements using pulsed lasers are feasible and can be used for the study of highly fluctuating flows and in facilities where the available measurement time is brief. Only a few molecules can be used for PLIF diagnostics in the reaction zone of H_2-air flames. Oxygen is an excellent candidate for diagnostics in nonreacting flows[3] or in fuel-lean flames. However, it is consumed in stoichiometric or fuel-rich flames. An alternative molecule for diagnostics both in the mixing and the reaction zones is NO (Ref. 4). However, artificial seeding of NO may be required, thereby perturbing the reaction chemistry.

The OH molecule is a naturally occurring molecule in the reaction zone, relatively stable and sufficiently abundant for PLIF measurements. Therefore, it can be selected for measurements of the flame temperature or the flow velocity. Furthermore, the density distribution of the hydroxyl radical is readily available by PLIF and is one of the many parameters needed to validate numerical codes used to simulate supersonic mixing and combustion. However, interpretation of the measurements obtained using certain laser-based techniques may strongly depend on facility characteristics. Parameters for the selection of a laser technique for diagnostics in scramjet testing facilities were evaluated and selection criteria are presented.

Presented as Paper 92-0508 at the AIAA 30th Aerospace Sciences Meeting, Reno, NV, Jan. 6–9, 1992; received March 16, 1992; revision received July 29, 1992; accepted for publication July 29, 1992.

*Research Assistant, Aerospace Research Laboratory. Student Member AIAA.

†Associate Professor, Aerospace Research Laboratory. Member AIAA.

‡Research Associate Professor, Aerospace Research Laboratory. Member AIAA.

Five primary types of facilities are currently available for scramjet testing.[1] Four of these types of facilities, the vitiated air, electric-arc heated air, pebble-bed, and the electrical-resistance heated air facilities, allow testing at flight Mach numbers to approximately 8 and total temperatures to approximately 2000 K. In the fifth type, pulsed shock tunnel facilities, gases upstream of the flame region may reach static temperatures on the order of 2800 K, providing true enthalpy testing to flight Mach numbers of 20 (Ref. 5). In all of these facilities, the measurements of temperature and density of OH are considered valuable for validation of the codes that simulate the mixing and reaction of H_2 in air. However, characteristics of high-speed flows and of large-scale facilities may introduce significant systematic errors that cannot be corrected without a full knowledge of the local flow composition, velocity, and temperature. These characteristics may include the following: strong gradients in pressure, temperature, and concentration; high concentration of water vapor or other quenching species; Doppler shift of the absorption frequency; and optically thick medium for both incident and emitted radiation. Therefore, the extent of these systematic errors, which are additive to the noise-induced uncertainty, must be estimated as part of the design of PLIF systems for imaging OH distributions quantitatively.

Several laser systems are available for the excitation of ro-vibronic transitions in the $A^2\Sigma^+ \leftarrow X^2\Pi$ band of OH. Owing to the high population density in the ground vibrational state most PLIF schemes call for the excitation of molecules from $v'' = 0$. However, the selection of the target vibrational level v' depends on the experimental requirements and the available laser system. The largest Einstein B coefficient in this manifold is for a $v' = 0 \leftarrow v'' = 0$ ro-vibronic absorption.[6] From there the Einstein B coefficient decreases rapidly as v' increases. Therefore, LIF applications are usually limited to excitations of $v' \leq 3$.

A dye laser, following frequency doubling or mixing, can be tuned to a resonance with any ro-vibronic transition in the 0, 1, 2, 3←0 bands. A XeCl excimer laser is resonant only with ro-vibronic transitions in the 0←0 band and a KrF excimer laser is resonant only with ro-vibronic transitions in the 3←0 band.

Ro-vibronic transitions in the 0←0 band may be excited by both a frequency doubled dye[7] and XeCl excimer lasers.[8] Most of the subsequent fluorescence is re-emitted in the 0→0 or 0→1 bands, yielding an intense signal. Owing to the strong absorption in the 0←0 band, the incident laser beam is attenuated significantly and the emitted fluorescence is reabsorbed, or trapped even in small-scale laboratory facilities.[8] This absorption and trapping resulted in an observable distortion of

the PLIF images.[8] Therefore, the excitation of this band by either the XeCl laser or the doubled-dye laser is precluded for applications in scramjet testing facilities where larger concentration of OH and larger dimensions are expected.

Alternatively, the doubled-dye laser system, with typical pulse energies of 40 mJ can be tuned to resonance with ro-vibronic transitions in the 1←0 band.[9] The subsequent fluorescence, like the absorption, is also relatively strong.[10] However, like the 0←0 excitation, the strong absorption can lead to attenuation of the incident beam and trapping of the emitted radiation in flows of even moderate OH concentration. The lifetime of the $v' = 1$ state is long ($\sim 10^{-6}$s) (Ref. 6) relative to the typical intermolecular collision time in test facilities ($\sim 10^{-9}$s). Thus many collisions can occur before fluorescence is emitted, thereby quenching the excited electronic state significantly. Correcting for beam attenuation, fluorescence trapping, and collisional quenching requires prior knowledge of local temperature and species concentration.

The $A^2\Sigma^+(v' = 2) \leftarrow X^2\Pi(v'' = 0)$ band can also be excited by the doubled-dye laser. The extent of beam attenuation by absorption is greatly reduced. The effect of fluorescence trapping may also be reduced by limiting the detection of the fluorescence to the 2→2 and 2→1 bands. However, since the detection is limited only to radiation emitted from $v' = 2$ removal of molecules from that level by either vibrational or electronic quenching will influence the measurements. Correction for these two different quenching effects may prove to be difficult.

The absorption in the 3←0 band is 100 times weaker than the 1←0 band absorption and the excited $v' = 3$ state is strongly predissociated with a characteristic lifetime of 100 ps (Ref. 11). Thus, the troublesome effects of beam attenuation, radiation trapping, and collisional quenching can be ameliorated relative to the excitation induced in the 1←0 band. However, this weak absorption and predissociation is accompanied by fluorescence yields that are considerably reduced relative to the 1←0 or 2←0 bands. Therefore, a KrF laser with pulse energy in excess of 240 mJ is required for the excitation of this band.[12]

It is evident that the selection of the most applicable laser technique involves an optimization in which the influence of the expected conditions in the test facility (e.g., pressure, OH density, temperature, and H_2O concentration) on several competing spectroscopic effects is considered. The restrictions on the application of the doubled-dye and KrF lasers for OH PLIF temperature and density measurements in various supersonic combustion facilities have been evaluated using a detailed spectral model of the LIF process of OH together with experimental results obtained in our supersonic high-temperature combustion facility[13] and measurements by others. Owing to the strong absorption and trapping associated with the excitation by a XeCl laser it was not evaluated for diagnostics in scramjet test facilities. The results are presented graphically to include the relevant design parameters and to cover the operational conditions of most supersonic combustion test facilities.

Theoretical Model

A computer model for the simulation of the LIF process in OH has been developed to predict the capabilities of the two laser systems that are used most often for OH imaging. The model includes three primary blocks that are used to predict 1) the spectral location of all of the relevant absorbing and emitting transitions, 2) the extent of absorption of the incident beam, and 3) the fluorescence yield and the extent of radiation trapping for typical laser and facility parameters.

To accurately simulate the interaction of the narrow-band tunable KrF laser or the frequency-doubled dye laser with OH, the model included all the OH vibronic transitions in the $A^2\Sigma^+(v' = 0, 1, 2, 3) \leftarrow X^2\Pi(v'' = 0, 1)$ band and rotational quantum numbers to $N \leq 30$. For absorption, only the transitions that are resonant with the incident laser beam were included. For emission, all the transitions that are transmitted through typical detection systems were included. Using the first block of the model and published spectroscopic coefficients[14] for the calculation of the term values, we obtained absorption and emission frequencies that matched experimental results[10] within 1 cm^{-1}.

The second block in the model included the calculation of the incident energy absorbed by OH. In addition to predicting the beam attenuation, this block is used to determine the density of the excited molecules. The energy dE, in Joules, lost from the incident beam due to absorption by a ro-vibronic transition from $v''N''$ to $v'N'$, when a laser pulse with an incident energy E_0 and a uniform spectral distribution over the absorption line width $\Delta\nu_{N''v'N'}$ cm^{-1} travels a distance dx, in centimeters, through a medium with an OH density N_{OH} cm^{-3}, and an Einstein B coefficient of $B_{N''v'N'}$ in $cm^3 - cm^{-1}$/(s-J) is given as[15]

$$dE = -E_0 N_{OH} \beta_{N''} \frac{B_{N''v'N'} h \nu_{N''v'N'}}{\Delta\nu_{N''v'N'}} dx \tag{1}$$

In Eq. (1), $\nu_{N''v'N'}$, is the frequency of the absorbing transition, $\beta_{N''}$ is the Boltzmann fraction of the molecules occupying the $v''N''$ level at a temperature T, and h, in Joules-second, is Planck's constant. Since all absorbing transitions in this work were from $v'' = 0$, the notation of Eq. (1) does not include v''. The incident energy E, after traveling a finite distance Δx, is then

$$E/E_0 = \exp[-N_{OH}\beta_{N''}\sigma_{N''v'N'}\Delta x] \tag{2}$$

where

$$\sigma_{N''v'N'} = \frac{B_{N''v'N'} h \nu_{N''v'N'}}{\Delta\nu_{N''v'N'}} \tag{3}$$

is the absorption cross section, in square centimeters.

The third block of the model includes calculation of the total number of photons emitted by the excited molecules and detected. To simulate realistic experiments, the collection was represented by a lens with a solid angle Ω, in steradian, and a bandpass filter with a transmission efficiency η_F that was selected to transmit radiation in the $v'v_f$ band. By also including the detector quantum efficiency η_D, the results could be presented in terms of photoelectrons emitted at each pixel in an imaging camera. This number does not include the amplification by an intensifier.

A typical imaging configuration where a section of length L along a laser light sheet is imaged onto a detector array with n_p rows and m_p pixels in each row is presented in Fig. 1. When the transverse distribution of laser energy is uniform, the

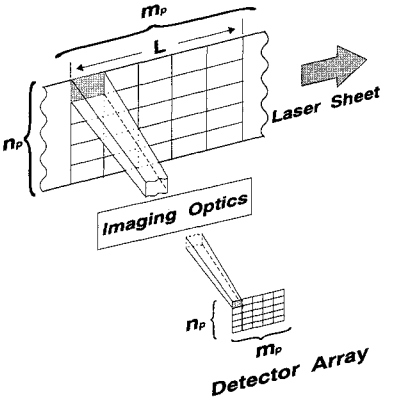

Fig. 1 Typical PLIF imaging configuration: section of a laser light sheet of length L is imaged onto a detector array with $m_p \times n_p$ pixels.

energy available for fluorescence excitation along each row decreases inversely with n_p and the energy term E_0 in Eqs. (1) and (2) is replaced with E_0/n_p. The differential length element dx in Eq. (1) corresponds in Fig. 1 to the length of an element in the flowfield, L/m_p, imaged by a single pixel.

The number of photoelectrons n_{pe}, emitted at each pixel of the detector array presented in Fig. 1 when imaging OH fluorescence induced in a H_2-air flame by a laser light sheet was calculated. Although a selected ro-vibronic state is excited, vibrational-vibrational energy transfer (VET) and rotational energy transfer (RET) may distribute the energy among other excited states. In addition, selection rules allow each vibrational and rotational state to decay, through radiative transfer, to several lower levels. Although our calculation considered all of these possibilities, the present notation indicates only $v'N'$ for the initial level and v_fN_f for the final state of the radiative transition. The number of photoelectrons n_{pe}, emitted by each imaged element is

$$n_{pe} = \left(\frac{\Omega}{4\pi}\eta_F\eta_D\right)\frac{E}{h\nu_{N''v'N'}n_p}N_{OH}\beta_{N''}\sigma_{N''v'N'}\frac{L}{m_p} \times \frac{A_{v'v_f}}{A_{ef} + P_{v'N'} + Q_{v'N'}} \quad (4)$$

In Eq. (4), $A_{v'v_f}$ s^{-1}, is the Einstein A coefficient for emission in the detected band; A_{ef} represents the effective Einstein coefficient obtained by the summation of the spontaneous-transition rates to all of the ground vibronic states; $P_{v'N'}$ s^{-1}, is the predissociation rate of the emitting level[11]; and $Q_{v'N'}$ s^{-1}, is the collisional-quenching rate that was calculated using the method in Ref. 16.

The collisional-quenching rate $Q_{v'N'}$ in Eq. (4) strongly depends on the concentration of the primary quenching partners OH, H_2O, H_2, O_2, and N_2, and the static temperature. However, the cross section for OH quenching by collisions with water vapor is approximately 100 times larger than the cross section for collisions with N_2 and approximately five times larger than the cross section for collisions with O_2 (Ref. 16). Therefore, in vitiated air facilities, where the inlet concentration of H_2O is high, the total quenching rate in the flow can be approximated by assuming collisions with H_2O only. From this, when $Q_{v'N'}$ is very large relative to both A_{ef} and $P_{v'N'}$, OH LIF measurements can be shown to produce semiquantitative images of the molar ratio of OH to H_2O even in the presence of large temperature, density, or gas composition variations.[17] Although our model can account for quenching by all of the major combustion species, we considered only the quenching by H_2O for the comparison of the performance of the tunable KrF laser with the doubled-dye laser system.

As a final test of our assembled model we calculated the excitation spectrum for the $A^2\Sigma^+(v' = 3) \leftarrow X^2\Pi(v'' = 0)$ band, of OH in a 1500 K flame, excited by a tunable KrF laser and detected through a spectrometer tuned to 329 nm with a resolution of 1 nm. The relative intensities in this spectrum compare very well with an experimental scan[12] obtained in similar conditions. In addition, we successfully compared the calculated dispersion spectrum with our own measurements which were obtained under similar conditions. The correct prediction of the relative strengths of the absorption lines and the emission lines confirms the ability of the model to predict the relative attenuation of the incident beam by the various lines and the relative fluorescence intensity expected at each wavelength.

Results

The criteria selected here for the evaluation of the doubled-dye laser and the tunable KrF laser are those that have the strongest influence on their performance. The first parameter that must be considered is the fluorescence yield. Only if the yield exceeds a required detection threshold will other criteria, such as beam attenuation or fluorescence trapping, be considered. Therefore, we present our results in the order of their priorities in the design process.

Fluorescence Yield

To evaluate the performance, based on the fluorescence yield criterion, of the two lasers most commonly used for OH LIF, we calculated the variation of the photoelectron count per pixel with N_{OH} at a static temperature of 2000 K, following excitation by each of these lasers without laser-beam attenuation or fluorescence trapping. Many OH absorption lines are resonant with doubled-dye lasers. However, since the typical pulse energy of this laser is much lower than the pulse energy of the KrF laser, only high-yield transitions, e.g., the $0\leftarrow0$, $1\leftarrow0$, or the $2\leftarrow0$ bands, are selected for planar imaging when the OH density is low. Although the absorption cross section of the $0\leftarrow0$ band is the largest, the $1\leftarrow0$ band is most commonly used[9] to reduce the effects of beam attenuation by absorption as will be discussed in the next section. The strong $1\leftarrow0$ $Q_1(6)$ primary absorption line and the weak $1\leftarrow0$ S_{21} (9) satellite line were selected to represent a typical range of $B_{N''v'N'}$ coefficients. The excitation by the tunable KrF laser was represented by the $3\leftarrow0$ $P_1(8)$ absorption. To simulate a realistic experiment, the following parameters were included in the calculation: a section of 1 mm^2 within a 100-mm-wide light sheet was imaged on each pixel, for which $\eta_D = 0.1$, through a lens with collection efficiency of 0.01 ($\sim f/2.5$), and a bandpass filter with $\eta_F = 0.1$. With resolution of 1 mm^2, turbulence analysis in large- and medium-scale facilities is possible. Equation (4) may be used to scale the present result for performance analysis when other resolution is required. A characteristic predissociation rate of 1.25×10^{10} s^{-1} was used[11] for the calculation of the fluorescence yield, using the tunable KrF laser system, whereas the quenching rate was neglected. On the other hand, when excitation by the doubled-dye laser was modeled, the predissociation rate was neglected. Instead, a collisional-quenching rate of $Q_{v'N'} = 5.76 \times 10^8$ s^{-1}, which is expected in a 30%-water-vapor air mixture at 1 atm and 2000 K (Ref. 16), was used. A laser line width of $\Delta\nu = 0.32$ cm^{-1} was selected. This line width overlaps the absorption line width defined by pressure and temperature broadening at 2000 K and 1 atm thereby efficiently coupling the incident energy with the absorbing transition. Furthermore, the narrow line width assures selective excitation of OH with no interaction with other combustion species such as O_2 and NO (Ref. 12). Excitation spectra of OH in H_2-air and H_2-O_2 flames using a narrow-band KrF laser obtained by Ref. 12 and by us showed no evidence of fluorescence from any other combustion species or from the photodissociation of H_2O by the intense uv radiation. In three-dimensional high-speed flows, broader laser lines may be required to allow for the Doppler shift introduced by flow velocity components along the incident beam.

Table 1 presents N_{OH} required to exceed a detection threshold of 100 photoelectrons/pixel and the signal that will be detected when $N_{OH} = 10^{16}$ cm^{-3}. Excitations by the doubled-dye laser included the primary and satellite $1\leftarrow0$ bands with detection in the $1\rightarrow1$ and $0\rightarrow0$ bands and excitation of the primary $2\leftarrow0$ band followed by detection in the $2\rightarrow1$ band. Excitation by the

Table 1 Minimum OH concentration required to exceed the detection threshold and the expected signal when $N_{OH} = 10^{16}$ cm^{-3} for several excitation and detection modes and when beam attenuation or fluorescence trapping are negligible

Laser system	Absorption transition	Emission band detected	Minimum N_{OH} cm^{-3}, for $n_{pe} \geq 100$	n_{pe} for $N_{OH} = 10^{16}$ cm^{-3}
Doubled dye	$1\leftarrow0$ $Q_1(6)$	$1\rightarrow1$ and $0\rightarrow0$	2.5×10^{12}	4.0×10^5
Doubled dye	$1\leftarrow0$ $S_{21}(9)$	$1\rightarrow1$ and $0\rightarrow0$	2.4×10^{13}	4.2×10^4
Doubled dye	$2\leftarrow0$ $Q_1(6)$	$2\rightarrow1$	2.0×10^{13}	5.0×10^4
Tunable KrF	$3\leftarrow0$ $P_1(8)$	$3\rightarrow2$	1.1×10^{15}	9.0×10^2
Tunable KrF	$3\leftarrow0$ $P_1(8)$	$3\rightarrow3$	5.0×10^{15}	2.0×10^2

tunable KrF laser included the 3←0 band followed by detection either in the 3→2 or 3→3 bands. When the threshold of 100 photoelectrons/pixel is exceeded, the photon-statistical rms noise is expected to be ≤ 10% of the total count.[18] This noise is believed to introduce the highest uncertainty that is still acceptable in most density, temperature, or velocity measurements. Based on this criterion, the signal generated by the doubled-dye laser system can exceed the 10% photon-noise threshold in most practical applications to supersonic combustion. The excitation by the tunable KrF laser exceeds the 10% photon-noise threshold when $N_{OH} > 10^{15}$ cm^{-3} for detection of the 3→2 fluorescence band, or when $N_{OH} > 3 \times 10^{15}$ cm^{-3} for 3→3 band detection. The results in Table 1 do not account for attenuation by absorption or trapping. When either of these effects is appreciable, the incident energy or N_{OH} may need to be increased to exceed the detection threshold.

Beam Attenuation and Fluorescence Trapping

As the density of OH increases, the optical thickness of the reacting mixture, as defined by Ref. 19, increases and both the incident beam and emitted fluorescence may be attenuated significantly. This has been observed in our supersonic, electrically heated combustion tunnel where transverse images of the OH distribution were obtained by the excitation of the 1←0 $Q_1(6)$ transition using a doubled-dye laser.[20] Despite the small size of the test section (~3 cm) and the moderate concentration of OH (~10^{15} cm^{-3}), the images were severely distorted both by absorption of the incident laser beam and by trapping of the emitted fluorescence. The extent of the absorption of the incident doubled-dye laser beam can be decreased by exciting a weaker absorption line. However, trapping of the emitted fluorescence will still remain a serious limitation. Attenuation by absorption and trapping, which is not affected by the transverse spatial distribution of the laser beam energy, is expected to become even more pronounced, for both laser systems, in large facilities or at high OH concentrations.

We determined theoretically the extent of attenuation of the doubled-dye and the tunable KrF laser beam as a function of OH concentration and optical path length. In most flames the OH density distribution is highly nonuniform and unsteady. However, attenuation is the result of an integration along the beam path. Therefore, attenuation can be accurately modeled by multiplying the average N_{OH} along the incident beam by the distance traveled by that beam through the absorbing medium. Figure 2 presents the variation of the normalized transmission of the beam, for a static temperature of 2000 K, with the line integral of the product of N_{OH} and the distance traveled by the incident beam through the absorbing medium. This parameter represents the number of OH molecules intercepted along the beam path per unit area. Included in the figure are the normalized attenuation of the doubled-dye laser beam, when exciting the 1←0 $Q_1(6)$ primary line and the 1←0 $S_{21}(9)$ satellite line, and the attenuation of the tunable KrF laser beam when exciting the 3←0 $P_1(8)$ transition—the strongest absorbing line within the tuning range of the laser. To facilitate comparison, the conditions for three typical supersonic combustion test facilities are marked on the abscissa. Accordingly, the General Applied Sciences Laboratory (GASL) direct connect module (DCM) vitiated tunnel is represented by an OH concentration of 1.5×10^{15} cm^{-3} and a characteristic dimension of 10 cm (Ref. 21). The University of Virginia (UVA) supersonic combustion tunnel is represented by a characteristic dimension of 5 cm and an OH concentration of 2×10^{15} cm^{-3} (Ref. 22). A typical pulsed scramjet test facility is represented by a characteristic dimension of 10 cm and a characteristic OH concentration of 10^{17} cm^{-3}. This latter concentration was calculated for an equilibrium mixture at a characteristic static temperature of 2800 K (Ref. 5).

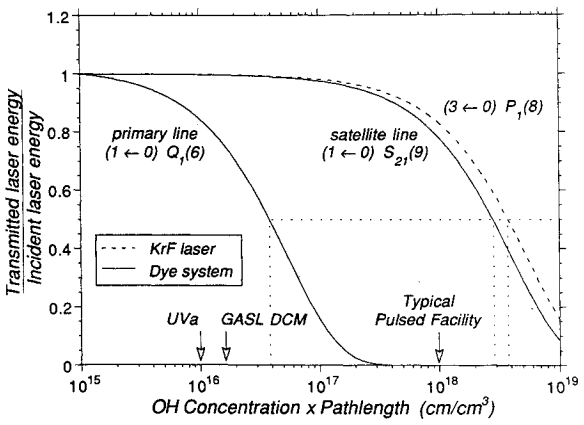

Fig. 2 Variation of the transmission with the number of OH molecules intercepted per unit area of the doubled-dye (solid line) or tunable KrF (dashed line) laser beams passing through reacting flow at static temperature of 2000 K; absorbing transitions and typical absorption depths in various facilities are indicated.

The attenuation, in Fig. 2, of the doubled-dye laser beam by the H_2-air flame in the GASL DCM and the UVA facilities is less than 50%. However, in typical pulsed facilities, where the concentration of OH is large, the doubled-dye laser beam will not penetrate the reacting flow when the laser is tuned to the primary, 1←0 $Q_1(6)$, transition. As an alternative, the laser may be tuned to the weaker satellite, 1←0 $S_{21}(9)$, line. (Use of this line involves other problems as pointed out subsequently.) As a second alternative, the more powerful KrF laser system may be used for diagnostics with a predicted attenuation of less than 20%, even in the pulsed facilities where N_{OH} is high. The higher pulse energy of this laser will partially compensate for the smaller fluorescence yield that accompanies the reduced absorption.

A related effect that can distort LIF measurements in hot gases is fluorescence trapping. When the radiative transition terminates at a low vibrational level and the temperature is high, the density of the population in the end state may be sufficient to re-absorb a large part of the LIF. Therefore, the detected fraction of the LIF emitted at a point depends on the integrated concentration and temperature of OH along the optical path to the detector from that point. If the temperature and concentration vary randomly, the fraction of the initial LIF detected will vary randomly as well.

When the $A^2\Sigma^+$, $v' = 1$ state is excited by the doubled-dye laser, only the fluorescence emitted by transitions to $v_f \geq 1$ can be spectrally separated from the incident radiation.[10] Of the many radiative bands, the 1→1 band is the brightest and is usually selected for detection by a bandpass filter centered around 310 nm (Ref. 9). However, owing to VET between the excited OH molecules and the major combustion species, a large fraction of the molecules initially in the $A^2\Sigma^+$, $v' = 1$ level decays to the $v' = 0$ level.[23] Radiation emitted in the 0→0 band cannot be spectrally discriminated by commercially available bandpass filters from the fluorescence in the 1→1 band. Since the transition probability in the 0→0 band is approximately twice as large as the probability for transition in the 1→1 band,[7] much of the imaged fluorescence will be in the 0→0 band. Although most of the trapping is expected in the 0→0 band, trapping in the 1→1 band is also likely to be significant. The extent of attenuation by trapping will depend on the rate at which excited molecules decay from $v' = 1$ to $v' = 0$ and on the temperature of the flame and OH concentration along the detection line-of-sight. Accounting for trapping would require complete knowledge of the temperature and OH concentration distribution within the laser beam and the imaging cone. Therefore, avoidance of trapping is essential in the design of an LIF diagnostics procedure.

In contrast, the excitation by the tunable KrF laser involves transition to the $A^2\Sigma^+$, $v' = 3$ level from which radiation is detected either in the 3→3 or 3→2 band. VET from $v' = 3$ is limited by the strong predissociation. Measurements in our H_2-air flat flame burner at a temperature of 1500 K and

pressure of 0.3 atm showed that the depletion of the $v' = 3$ state by VET is less than 3%. We also demonstrated that fluorescence in the 0→0 and 1→1 bands, which follow this slight VET, can be spectrally discriminated from the 3→3 and 3→2 bands by a commercially available bandpass filter. When the static temperature is 2000 K, the population in $v_f = 2$ is 0.7% of N_{OH} and in $v_f = 3$ is only 0.06%. Therefore, trapping by the $X^2\Pi$, $v_f = 2$ and 3 levels is significantly less than by the $v_f = 0$ and 1 levels.

Figure 3 presents the ratio of detected to emitted fluorescence with the number of OH molecules intercepted, per unit area, along the detection path. The number of intercepted OH molecules was calculated for the three representative facilities using the same uniform N_{OH} distribution as in Fig. 2, and a characteristic path of 10 cm for the GASL and scramjet facilities. A characteristic path of 25 cm was selected for the UVA facility to simulate the imaging conditions of Ref. 20. As before, the dye laser is represented by excitations in the 1←0 $Q_1(6)$ and the satellite 1←0 $S_{21}(9)$ bands. Two humps are apparent in each of these curves. The upper hump is due to fluorescence trapping in the 0→0 band. The lower hump, due to the fluorescence trapping in the 1→1 band, becomes apparent only after the radiation in the 0→0 band is depleted. Despite the low attenuation of the incident beam when it is tuned to the satellite band, the effect of trapping is similar to that experienced when the primary band is excited. In applications involving the GASL DCM facility, the effect of trapping is moderate. However, even in a small facility, like the UVA combustion tunnel, where a larger detection path length is used, trapping is significant and may cause a nonuniform signal loss of as much as 70%. Clearly, the signal generated by the doubled-dye laser in the pulsed scramjet facility can be fully trapped. Thus, although the beam may penetrate the flow when the laser is tuned to the satellite transition, no signal will be detected if the optical path length is too long.

A possible strategy for reducing the trapping of the fluorescence using the dye laser system is excitation of the 2←0 band. Subsequent fluorescence in the 2→1 band may be spectrally resolved from fluorescence in the 0→0, 1→1, and possibly the 1→0 bands emitted by molecules that decayed from $v' = 2$ to the $v' = 1$ and $v' = 0$ levels by VET. The calculated trapping of the fluorescence in the 2→1 band is also presented in Fig. 3. Excitation on the 2←0 $Q_1(6)$ line was selected to facilitate comparison with excitation on the primary, 1←0 $Q_1(6)$ line. This result suggests that fluorescence trapping may be significantly reduced if fluorescence from $v' = 2$ can be successfully isolated from fluorescence from $v' = 1$ and $v' = 0$. However, if the isolation is successful, problems will still remain. Molecules removed from $v' = 2$ by VET will not contribute to the detected fluorescence. This is in contrast to the fluorescence induced by the excitation of the 1←0 band, which is insensitive to VET because the 1→1 and the 0→0 bands are detected simultaneously. The rates for VET[23] are most likely significant and are probably not dominated by collisions with H_2O as may occur in some cases with electronic quenching,[16] as mentioned earlier. To illustrate, the cross section for VET from $v' = 1$ for collision with N_2 at 300 K is 26 Å^2 (Ref. 23) whereas the cross section for electronic quenching by N_2 is only 2.5 Å^2 (Ref. 16). Conversely, the cross section for electronic quenching by H_2O is 76 Å^2 (Ref. 16) whereas for VET by H_2O is < 14 Å^2 (Ref. 23). Since the lifetime in the $v' = 2$ state is 50 ns or longer,[24] measurement of the fluorescence from $v' = 2$, in atmospheric pressure flames, will strongly depend on the local composition and temperature. This dependence is more complicated for $v' = 2$ than for $v' = 1$, where only electronic quenching must be considered and may be corrected.[25] This added complexity is expected to prevent quantitative OH density and temperature measurements using the 2←0 excitation in atmospheric pressure flames. At sufficiently low pressures, when the time between collisions exceeds the natural lifetime, quenching of $v' = 2$ will be negligible. However, at those conditions trapping of the fluorescence induced by the more efficient excitation of the 1←0 transition is also negligible. Therefore, no further consideration is made of the 2←0 excitation.

In contrast, Fig. 3 also shows the effects of fluorescence trapping for excitation by the tunable KrF laser. Two cases are presented: attenuation by trapping for radiative transitions to $X^2\Pi$, $v_f = 2$, and attenuation by trapping for radiative transitions to $X^2\Pi$, $v_f = 3$. As expected, the trapping by the $v_f = 2$ level of fluorescence in the 3→2 band is larger than the trapping by the $v_f = 3$ level. However, in most applications both transitions may be useful and the selection will be dominated by considerations of signal level and discrimination of the laser-induced OH fluorescence against chemiluminescence or competing LIF from other combustion species.

Figure 4 presents the variation with OH concentration of the combined effects of attenuation and trapping for the four modes of excitation and detection discussed earlier. For simplicity, the absorption and trapping path lengths were considered to be 10 cm for the three representative facilities. The data of Table 1 and Fig. 4 show clearly that the doubled-dye laser system may be tuned to either the primary or the satellite excitation for measurements in the GASL DCM facility. However, the detected fluorescence will be severely attenuated in the pulsed scramjet facilities. On the other hand, Table 1 and Fig. 4 demonstrate that the tunable KrF laser system is ex-

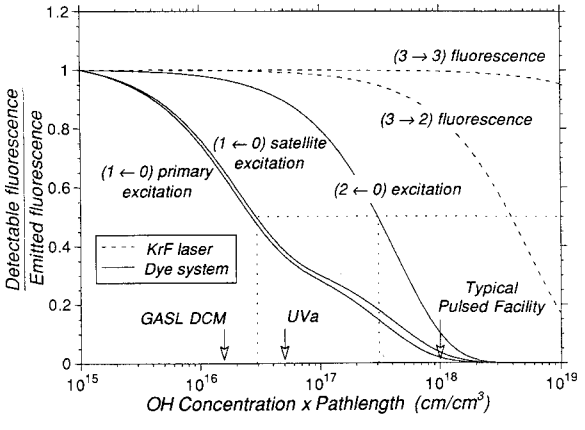

Fig. 3 Variation of the ratio of detected to emitted fluorescence, with the number of OH molecules intercepted, per unit area, along the detection path, for fluorescence induced by doubled-dye (solid line) and tunable KrF (dashed line) laser beams in reacting flow at static temperature of 2000 K; absorbing transitions for the dye laser and typical absorption depths in three scramjet test facilities are indicated, together with the detected bands, following excitation by dye and KrF laser systems.

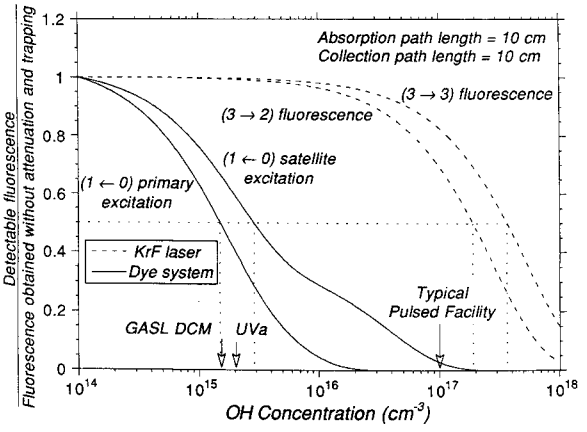

Fig. 4 Variation of the combined attenuation and fluorescence trapping effects with N_{OH} for doubled-dye (solid line) and tunable KrF (dashed line) laser beams passing through reacting flow at a static temperature of 2000 K: conditions are the same as in Figs. 2 and 3.

pected to be useful in all three facilities at concentrations above about 10^{15} cm^{-3}.

Collisional Quenching of Fluorescence

Collisional quenching is a source of systematic error in most LIF measurements. The error may be severe when the radiative lifetime of the excited state is long, relative to the time between collisions, and when the composition of the collisional partners varies widely. The radiative lifetime of the states excited by the doubled-dye laser system is approximately 1 μs (Ref. 6). This is more than 1000 times the time between collisions at atmospheric conditions. Therefore, unless corrections are made, collisional quenching will introduce a major source of error in applications of the dye laser system. Conditions where corrections for collisional quenching may not be necessary have been discussed previously.[25] However, measurements in supersonic combustion facilities, where large pressure and temperature gradients exist, will require corrections that will depend on the local densities of the major species and their temperatures. This detailed information is presently beyond the scope of diagnostic techniques and is not likely to be available in the near term.

To illustrate the effect of collisional quenching, we calculated the fluorescence signal upstream and downstream of an oblique shock wave in a hypothetical $M = 10$, stoichiometric, reacting H_2-air flow. The parameters selected for this calculation were well within the operating range of most pulsed facilities.[1] The oblique shock was assumed to be formed by a 5-deg compressive turn with an upstream static temperature of 1200 K and static pressure of 0.5 atm and predicted downstream conditions of $M = 8.5$, $T = 1730$ K, and $P = 1.5$ atm. Given that in the vicinity of the shock the flow is chemically frozen, the density of OH increases across the shock by a factor of 2.15. Therefore, according to Eq. (4), in the absence of collisional quenching, the LIF signal past the shock should also increase by a factor of 2.15. However, the simulated fluorescence intensity, following the excitation of the 1←0 $Q_1(6)$ line by the doubled-dye laser increases across the shock by only a factor of 1.06 when the effect of collisional quenching is included. This predicted fluorescence is nearly 50% of the increase by a factor of 2.15 that would be expected from the increase in N_{OH}. The increase in fluorescence due to an increase in N_{OH} behind the shock was offset here by an increase in the quenching losses. Thus, if the structure of this hypothetical flow was to be imaged using this technique, the fluorescence variation across the shock will be near or within the noise. On the other hand, the fluorescence induced by the tunable KrF laser system, following excitation of the 3←0 $P_1(8)$ line, would increase behind the shock by a factor of 2.29. Using the fluorescence intensity ratio as a measure of the OH density ratio across the shock, without corrections for collisional quenching and change in the Boltzmann fraction due to the temperature increase across the shock, the error, relative to the predicted OH density ratio of 2.15, is less than 7%. If the molecular number density is increased, the quenching rate would eventually approach the predissociation rate, and correction for quenching would be required. However, the preceding example is representative of most scramjet combustor conditions.

Owing to the high collisional electronic quenching cross section of OH with H_2O (Ref. 16), when water vapor is a major specie, corrections for collisional quenching may be simplified by neglecting the contribution of the other major species. Vitiated air flow presents a case in which the concentration of H_2O is large both upstream of the reaction zone and behind it. Therefore, if the vitiation mole fraction is large enough in a vitiated air-flow facility, correction for collisional quenching will require only the measurement of the concentration of H_2O. Figure 5 presents the calculated variation, with vitiation mole fraction, of the quenching rate by H_2O relative to the combined quenching rate by all major species following the excitation of the $A\,^2\Sigma^+$, $v' = 1$ state. Quenching both for the freestream conditions, without reaction, and the postflame regions were calculated. In the postflame region, quenching by H_2O accounts for more than 95% of the total, independent of the vitiation conditions. However, in the preflame region, the quenching rate by H_2O exceeds the quenching rate by the remaining air components only when the vitiation mole fraction exceeds 5%. This can be considered as a threshold above which quenching corrections may be simplified when the doubled-dye laser is used for LIF diagnostics of OH.

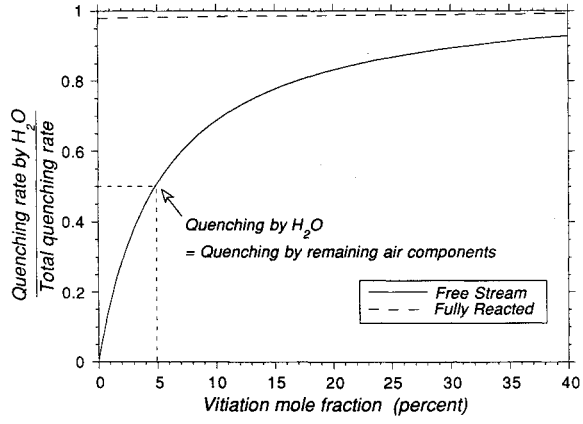

Fig. 5 Variation with vitiation mole fraction of the collisional quenching rate of the $A\,^2\Sigma^+$, $v' = 1$ state by H_2O vapor relative to the total collisional quenching rate: quenching in the freestream immediately ahead of the flame front (solid line), quenching behind the flame front (dashed line).

Laser System Application Charts

The previous results delineate the limits within which the doubled-dye and the tunable KrF laser systems can be applied with relatively small systematic errors and at signal levels sufficient for low-noise imaging. To summarize these results we present these limits graphically for both laser systems in Figs. 6 and 7. These charts may be used for the design of OH diagnostics experiments. The combustors for which this selection is required are characterized by the freestream vitiation mole-fraction; characteristic OH density; laser beam path length, which is the distance traveled by the incident laser beam through reacting flow; and a detection path length over which the emitted fluorescence travels to the detector.

Figure 6 presents a chart of the application limits for the doubled-dye laser system for OH diagnostics in reacting flows at a static temperature of 2000 K. This temperature is achievable in most scramjet test facilities. Therefore, the results presented in this figure may serve as a guideline for most design applications. The ordinate presents the number of OH molecules intercepted, per unit area along the laser beam, and the abscissa represents OH molecules intercepted, per unit area along the detection optical path. The hatched region marks the domain within which the excitation of the primary line experiences losses due to absorption and trapping that are below 50%. The dotted region marks the limits within which the excitation of the satellite line will meet the same restrictions. The low-end limit of both regions is determined by the condition that the detectable signal exceeds 100 photoelectrons/pixel. This limit defines a minimum concentration which needs to be exceeded for low-noise detection. Note that the limits of the dotted region are to the right of the hatched region. To simplify the corrections for collisional quenching, a minimum of 5% of freestream vitiation is required. With that level of vitiation, quenching by H_2O accounts for more than 50% of the total quenching rate (Fig. 5). The GASL DCM is the only facility shown in Fig. 6, since it is the only facility discussed here that exceeds the 5% vitiation requirement. The prediction made from this chart, that the doubled-dye laser is suitable for OH diagnostics in the GASL DCM

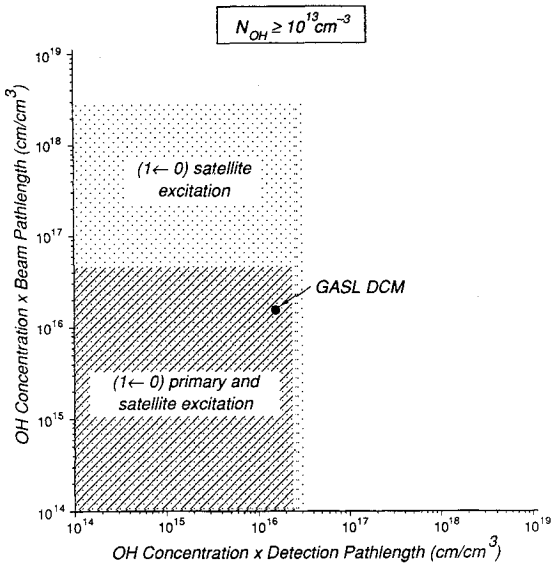

Fig. 6 Range of application of the dye laser system for OH diagnostics: application range for excitation of the 1←0 $Q_1(6)$ primary line (hatched area); application range for excitation of the 1←0 $S_{21}(9)$ satellite band (dotted area).

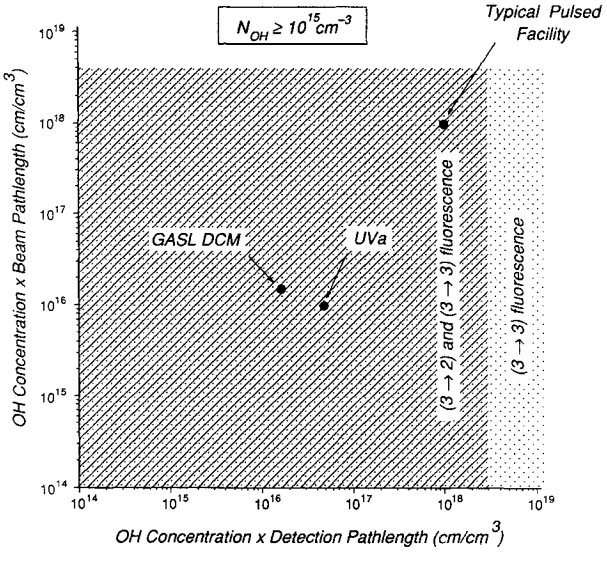

Fig. 7 Range of application of the tunable KrF laser system for OH diagnostics: 3→2 band (hatched area); 3→3 band (dotted area).

facility, has been confirmed previously by successful measurements.[21] Measurements in the nonvitiated UVA or pulsed facilities using the doubled-dye laser will require detailed knowledge of the concentration and temperature of all species to correct for quenching effects.

Figure 7 presents a chart of the application limits for the tunable KrF laser system for OH diagnostics in reacting flows at a static temperature of 2000 K. The hatched region represents excitation to the $A^2\Sigma^+$, $v' = 3$ level followed by detection in the brighter 3→2 band. The dotted region represents the same excitation followed by detection in the less efficient 3→3 band. The conditions in all of the facilities considered here fall within the application limits of either the 3→2 detection or the 3→3 detection. Thus, the tunable KrF laser system may be used for OH diagnostics in most existing supersonic combustion facilities. In particular, it is expected to be the only existing light source for quantitative planar OH concentration measurements in high-temperature, large-scale test facilities. The usefulness of the tunable KrF laser system is limited by the low fluorescence yield, to facilities where $N_{OH} > 10^{15}$ cm^{-3}.

Conclusions

The objectives of this work were 1) to evaluate the performance of frequency-doubled-dye laser systems and tunable KrF laser systems for OH measurements in supersonic combustion facilities, and 2) to determine conditions in which each laser system may be used with relatively small systematic errors and with sufficient signal level for low-noise measurements.

A LIF model of OH was developed that incorporates all of the physical processes that are believed to be significant, including predissociation and collisional quenching. The model was validated by comparing calculated spectra with previously reported spectra and spectra obtained by us. The features investigated included the minimum local conditions necessary for applicable fluorescence signal for several excitation and detection schemes, the attenuation of the incident laser beam by absorption for both the dye laser and tunable KrF laser excitation, radiation trapping of the emitted fluorescence, and collisional quenching of the excited OH molecules.

Charts that delineate the application ranges for both laser systems were presented. The results show that the doubled-dye laser system is the most effective laser system for OH diagnostics when the concentration of OH is below 10^{15} cm^{-3}. When the KrF laser system is used for OH density measurements in combustor flows at static pressure as high as 1.5 atm, the correction for collisional quenching is less than 7%. In contrast, the local collisional quenching correction when the doubled-dye laser system is used at local static pressures around 1.5 atm is about 50%. However, when the level of freestream vitiation exceeds 5%, correction for collisional quenching of the OH molecules excited by the dye laser system require only knowledge of the local H_2O concentration. When the path integral of the OH concentration along the incidence or detection path lengths exceeds 10^{16} cm/cm^3, the KrF laser must be used to avoid attenuation by absorption or trapping. The signal induced by the KrF laser system at these conditions is usually sufficient for low-noise, high-resolution imaging.

Acknowledgments

The work of T. M. Quagliaroli was supported by the NASA Graduate Student Research Program Contract NGT-S0714. The authors are grateful to William B. Watkins at Pratt & Whitney, West Palm Beach, FL, for many helpful comments that led to this work.

References

[1]Chapman, G. T., "An Overview of Hypersonic Aerothermodynamics," *Communication in Applied Numerical Methods,* Vol. 4, May-June 1988, pp. 319-325.

[2]Eckbreth, A. C., *Laser Diagnostics for Combustion Temperature and Species,* Abacus Press, Cambridge, MA, 1988, pp. 301-362.

[3]Laufer, G., McKenzie, R. L., and Fletcher, D. G., "Method for Measuring Temperature and Densities in Hypersonic Wind Tunnel Air Flows Using Laser-Induced O_2 Fluorescence," *Applied Optics,* Vol. 29, Nov. 1990, pp. 4873-4883.

[4]Cattolica, R. J., Cavolowsky, J. A., and Mataga, T. G., "Laser-Fluorescence Measurements of Nitric Oxide in Low-Pressure H_2/O_2/NO Flames," *22nd Symposium (International) on Combustion,* Seattle WA, Aug. 1988, pp. 1165-1173.

[5]Rogers, R. C., "Workshop on The Application of Pulse Facilities to Hypervelocity Combustion Simulation," National Aero-Space Plane Workshop Publ. 1008, Monterey, CA, 1990.

[6]Dimpfl, W. L., and Kinsey, J. L., "Radiative Lifetime of OH($A^2\Sigma^+$) and Einstein Coefficients for the A-X System of OH and OD," *Journal of Quantitative Spectroscopy and Radiative Transfer,* Vol. 21, No. 3, 1979, pp. 233-241.

[7]Kychakoff, G., Howe, R. D., Hanson, R. K., and McDaniel, J. C., Jr., "Quantitative Visualization of Combustion Species in a Plane," *Applied Optics,* Vol. 21, Sept. 1982, pp. 3225-3227.

[8]Seitzmann, J., Paul, P., and Hanson, R., "PLIF Imaging Analysis of OH Structures in a Turbulent Nonpremixed H_2-Air Flame," AIAA Paper 90-0160, Jan. 1990.

[9]Dyer, M. J., and Crosley, D. R., "Two-Dimensional Imaging of OH Laser-Induced Fluorescence in a Flame," *Optics Letters,* Vol. 7, Aug. 1982, pp. 382–384.

[10]Dieke, G. H., and Crosswhite, "The Ultraviolet Bands of OH Fundamental Data," *Journal of Quantitative Spectroscopy and Radiative Transfer,* Vol. 2, Jan. 1962, pp. 97–199.

[11]Gray, J. A., and Farrow, R. L., "Predissociation Lifetimes of OH $A^2\Sigma^+(v' = 3)$ Obtained from Optical-Optical Double-Resonance Linewidth Measurements," *Journal of Chemical Physics,* Vol. 95, Nov. 1991, pp. 7054–7060.

[12]Andresen, P., Bath, A., Gröger, W., Lülf, H. W., Meijer, G., and ter Meulen, J. J., "Laser-Induced Fluorescence with Tunable Excimer Lasers as a Possible Method for Instantaneous Temperature Field Measurements at High Pressures: Checks With an Atmospheric Flame," *Applied Optics,* Vol. 27, Jan. 1988, pp. 365–378.

[13]Krauss, R. H., McDaniel, J. C., Jr., Scott, J. E., Jr., Whitehurst, R. B., III, Segal, C., Mahoney, G. T., and Childers, J. M., IV, "Unique, Clean-Air Continuous-Flow, High-Stagnation-Temperature Facility for Supersonic Combustion Research," AIAA Paper 88-3059, Boston, MA, July 1988.

[14]Moore, E. A., and Richards, W.G., "A Reanalysis of the $A^2\Sigma^+ - X^2\Pi_i$ System of OH," *Physica Scripta,* Vol. 3, No. 5, 1971, pp. 223–230.

[15]Herzberg, G., *Molecular Spectra and Molecular Structure I. Spectra of Diatomic Molecules,* R. E. Krieger, Malabar, FL, 1989, pp. 20–21.

[16]Barlow, R. S., Dibble, R. W., and Lucht, R. P., "Simultaneous Measurement of Raman Scattering and Laser-Induced OH Fluorescence in Nonpremixed Turbulent Jet Flames," *Optics Letters,* Vol. 14, March 1989, pp. 263–265.

[17]Allen, M. G., Parker, T. E., Reinecke, W. G., Legner, H. H., Foutter, R. R., Rawlins, W. T., and Davis, S. J., "Instantaneous Temperature and Concentration Imaging in Supersonic Air Flow Behind a Rear-Facing Step with Hydrogen Injection," AIAA Paper 92-0137, Jan. 1992.

[18]Marcuse, D., *Engineering Quantum Electrodynamics,* Harcourt, Brace, and World, New York, 1970.

[19]Vincenti, W. G., and Kruger, C. H., Jr., *Introduction to Physical Gas Dynamics,* R. E. Krieger, Malabar, FL, 1982, p. 480.

[20]Abbit, J. D., III, Whitehurst, R. B., III, Segal, C., McDaniel, J. C., Jr., and Krauss, R. H., "Flowfield Visualization Study of a Supersonic Combustor," AIAA Paper 92-0090, Reno, NV, Jan. 1992.

[21]Davis, J. A., private communication, Rockwell International Corp., Rocketdyne Division, Canoga Park, CA, 1991.

[22]Segal, C., "Experimental and Numerical Investigation of Hydrogen Combustion in Supersonic Flow," Ph.D. Dissertation, Univ. of Virginia, Charlottesville, VA, Aug. 1991.

[23]Copeland, R. A., Wise, M. L., and Crosley, D. R., "Vibrational Energy Transfer and Quenching of OH ($A^2\Sigma^+$, $v' = 1$)," *Journal of Physical Chemistry,* Vol. 92, No. 20, pp. 5710–5715.

[24]Sink, M. L., Bandrauk, A. D., and Lefebvre, R., "Theoretical Analysis of the Predissociation of the $A^2\Sigma^+$ State of OH," *Journal of Chemical Physics,* Vol. 73, Nov. 1980, pp. 4451–4459.

[25]Barlow, R. S., and Collignon, A., "Linear LIF Measurements of OH in Nonpremixed Methane-Air Flames: When are Quenching Corrections Unnecessary," AIAA Paper 91-0179, Reno, NV, Jan. 1991.